Al–Mg DISORDER IN A GEM-QUALITY PARGASITE FROM BAFFIN ISLAND, NUNAVUT, CANADA

KIMBERLY T. TAIT AND FRANK C. HAWTHORNE[§]

Department of Geological Sciences, University of Manitoba, Winnipeg, Manitoba R3T 2N2, Canada

GIANCARLO DELLA VENTURA

Dipartimento di Scienze Geologiche, Università di Roma Tre, Largo S. Leonardo Murialdo 1, I-00146 Roma, Italy

ABSTRACT

The crystal structure of gem-quality pargasite from Soper River, near Kimmirut, Baffin Island, Nunavut, Canada, $(K_{0.24}Na_{0.73})_{\Sigma 0.97}$ $(Ca_{1.86}Na_{0.14})_{\Sigma 2.00}$ $(Mg_{4.15}Fe_{0.07}Mn_{0.01}Al_{0.71}Ti_{0.06})_{\Sigma 5.00}$ $(Si_{6.45}Al_{1.55})$ O_{22} $[(OH)_{1.25}F_{0.63}O^{2-}_{0.12}]_{\Sigma 2.00}$, a 9.8814(6), b 17.967(1), c 5.2927(4) Å, β 105.263(5)°, V 906.5 Å^3, C2/m, $Z = 2$, has been refined to an R index of 2.9% using 1506 observed intensities measured with Mo$K\alpha$ X-radiation. The crystal used for collection of the X-ray intensity data was then analyzed with an electron microprobe. The amphibole composition is very close to that of end-member pargasite. There is significant disorder of Al over the M(2) [1.40 Mg + 0.54 Al + 0.06 Fe^{3+}] and M(3) [0.81 Mg + 0.17 Al + 0.02 Fe^{2+}] sites. Such disorder has been observed in Mg-rich pargasite from a high-pressure paragenesis in the western Alps. The infrared spectrum of this amphibole in the principal OH-stretching region shows a complex envelope that can be resolved into six bands by analogy with the spectra of synthetic (OH,F)-bearing pargasite in the literature. The relative intensities of the component bands are in accord with the observed OH:F ratio in this pargasite, and indicate complete short-range disorder of OH and F. The occurrence of Al–Mg disorder over M(2) and M(3) in the Soper River pargasite, from a lower-pressure environment, indicates that this disorder is a compositional feature of pargasite, rather than a result of crystallization or equilibration at high pressure and temperature. The pattern of electron density in the A cavity of the structure may be interpreted in terms of K and Na at the A(m) site and Na at the A(2) site. Moreover, the specific site-populations are conformable with the composition of this amphibole and the most favorable patterns of short-range order.

Keywords: amphibole, pargasite, crystal-structure refinement, electron-microprobe analysis, Kimmirut, Baffin Island, Nunavut, Canada.

SOMMAIRE

Nous avons affiné la structure cristalline d'un échantillon de pargasite gemme de la rivière Soper, près de Kimmirut, île de Baffin, Nunavut, Canada, $(K_{0.24}Na_{0.73})_{\Sigma 0.97}$ $(Ca_{1.86}Na_{0.14})_{\Sigma 2.00}$ $(Mg_{4.15}Fe_{0.07}Mn_{0.01}Al_{0.71}Ti_{0.06})_{\Sigma 5.00}$ $(Si_{6.45}Al_{1.55})$ O_{22} $[(OH)_{1.25}F_{0.63}O^{2-}_{0.12}]_{\Sigma 2.00}$, a 9.8814(6), b 17.967(1), c 5.2927(4) Å, β 105.263(5)°, V 906.5 Å^3, C2/m, $Z = 2$, jusqu'à un résidu R de 2.9% en utilisant 1506 intensités observées, mesurées avec rayonnement Mo$K\alpha$. Le cristal a ensuite été analysé avec une microsonde électronique. La composition de l'amphibole est très proche de celle du pôle pargasite. Il y a un désordre important des atomes Al sur les sites M(2) [1.40 Mg + 0.54 Al + 0.06 Fe^{3+}] et M(3) [0.81 Mg + 0.17 Al + 0.02 Fe^{2+}]. Un tel désordre avait déjà été signalé dans un échantillon de pargasite magnésienne provenant d'une paragenèse équilibrée à plus haute pression dans les Alpes occidentales. Le spectre de cet échantillon dans l'infra-rouge, dans l'intervalle de l'étirement principal des groupes OH, montre une enveloppe complexe que nous pouvons résoudre en six bandes par analogie avec le spectre de la pargasite (OH, F) synthétique déjà dans la littérature. Les intensités relatives de ces bandes concordent avec le rapport OH:F observé dans cet échantillon, et indiquent un désordre complet à courte échelle de OH et F. La présence d'un désordre Al–Mg sur les sites M(2) et M(3) dans la pargasite de la rivière Soper, équilibrée à plus faible pression, indique que le désordre dépend de la composition de la pargasite plutôt que sa cristallisation ou son équilibrage à pression et à température élevées. Nous interprétons la distribution de la densité des électrons dans la cavité A de la structure en termes de l'occupation du site A(m) par K et Na, et du site A(2) par le Na. De plus, la distribution des atomes sur les divers sites est conforme à la composition de cette amphibole et aux exigences d'une mise en ordre à courte échelle.

(Traduit par la Rédaction)

Mots-clés: amphibole, pargasite, affinement de la structure cristalline, analyse à la microsonde électronique, Kimmirut, île de Baffin, Nunavut, Canada.

[§]   *E-mail address*: frank_hawthorne@umanitoba.ca

INTRODUCTION

Baffin Island is situated north of the province of Quebec, in the newly formed Nunavut Territory. Wight (1986) reported the occurrence of gem-quality "hornblende" in marbles along the Soper River (Grice & Gault 1983), 15 km north of Lake Harbour (now named Kimmirut). The analytical data given by Wight (1986) pertain to material described as "pargasitic hornblende" and "edenitic hornblende". The amphibole in this suite is of considerable interest as it has a low Fe content. Oberti *et al.* (1995) showed that in pargasite, there is some (Mg,Al) disorder over the *M*(2) and *M*(3) sites that increases with increasing Mg content. The amphibole of Soper River is highly magnesian, but was formed at a temperature and pressure significantly lower than was the case for pargasite of the Finero ultramafic complex characterized by Oberti *et al.* (1995). Examination of the Soper River amphibole allows us to test the suggestion of Oberti *et al.* (1995) that (Mg,Al) disorder in pargasite at Finero is induced by the chemical composition of the amphibole, rather than the high temperature and pressure of formation. The crystal used in this study is near end-member pargasite, whereas "pargasitic hornblende" and "edenitic hornblende" have been described previously from the same locality by Wight (1986).

EXPERIMENTAL

The crystal used in this investigation is from the Soper River locality near Kimmirut, Baffin Island, Nunavut, Canada. Gem rough was generously donated for this work by Brad Wilson, Kingston, Ontario.

X-ray diffraction

A fragment of a gem-quality crystal was attached to a glass fiber and mounted on a Siemens *P*4 automated four-circle diffractometer equipped with a graphite monochromator and Mo*K*α X-radiation. Cell dimensions (Table 1) were determined from least-squares refinement of the setting angles of fifty automatically aligned reflections in the range $20 < 2\theta < 40°$. Intensities were measured from 4 to 60°2θ ($\bar{1}3 \leq h \leq 13$, $0 \leq k \leq 14$, $0 \leq l \leq 13$) with scan speeds varying between 3.0

and 29.3°2θ/min; a total of 1506 reflections was measured over one asymmetric unit. Psi-scan data were measured for sixteen reflections uniformly distributed between 4 and 60°2θ, and an empirical absorption-correction was applied; we modeled the crystal as a triaxial ellipsoid. Intensities were corrected for Lorentz, polarization and background effects, and then reduced to structure factors; of the 1375 unique reflections, 1174 were classed as observed ($|F_o| > 5\sigma F$).

Structure refinement

All calculations were done with the SHELXTL PC (Plus) system of programs; *R*-indices are of the form given in Table 1 and are expressed as percentages. The structure refined rapidly to an *R* index of 2.9% for a model with anisotropic-displacement parameters for all sites except *A*(2) and *A*(*m*). The H atom was located in a difference-Fourier map, and its positional parameters were refined, subject to the soft constraint that the O(3)–H distance should be approximately 0.98 Å. Final atom coordinates and displacement factors are given in Table 2, refined site-scattering values are given in Table 3, and selected interatomic distances and angles are listed in Table 4. A structure-factor table may be obtained from the Depository of Unpublished Data, CISTI, National Research Council, Ottawa, Ontario K1A 0S2, Canada.

Electron-microprobe analysis

Subsequent to the diffraction experiment, the crystal used for collection of the X-ray intensity data was mounted in epoxy, ground, polished, carbon-coated and analyzed with a Cameca SX–50 electron microprobe. The crystal was analyzed in wavelength-dispersion mode at ten points and with the following conditions: excitation voltage: 15 kV, specimen current: 20 nA, beam size: 5 μm, peak count-time: 10 s, background count-time: 20 s. The mean chemical composition is given in Table 5, together with the unit formula calculated on the basis of 24 (O,OH,F), with OH + F = $2 - 2\ ^{M(1)}$Ti *apfu* (atoms per formula unit) (Oberti *et al.* 1992) and with all iron assumed to be divalent.

Infrared spectroscopy

Infrared spectra in the OH-stretching region of Soper River pargasite were collected on powder and single crystals. In the first case, the sample was prepared as a KBr pellet using the procedure of Robert *et al.* (1989). The spectrum was acquired with a Nicolet Magna 760 spectrophotometer equipped with a KBr beam-splitter and a DTGS detector; sixty-four spectra were averaged. In the second case, the unpolarized-light spectrum was collected at room temperature on a doubly polished fragment of a crystal (thickness 50 μm) using a Nicolet NicPlan microscope equipped with a KBr beam-splitter

TABLE 1. MISCELLANEOUS INFORMATION FOR
GEM-QUALITY PARGASITE

a (Å)	9.8814(6)	Crystal size (mm)	0.15 x 0.15 x 0.20
b (Å)	17.967(1)	Radiation/filter	Mo*K*α/graphite
c (Å)	5.2927(4)	Total Ref.	1506
β (°)	105.263(5)	*F* > 5σ*F*	1174
V (Å³)	906.51	Final *R*(obs) (%)	2.9
Space group	*C*2/*m*	Final *R*(all) (%)	3.8
Z	2		

$R = \Sigma(|F_o|-|F_c|)/\Sigma|F_o|$

$wR = [\Sigma w(|F_o|-|F_c|)^2/\Sigma F_o^2]^{1/2}$, $w = 1$

TABLE 2. FINAL POSITIONAL PARAMETERS AND DISPLACEMENT PARAMETERS ($Å^2 \times 10^4$) FOR GEM-QUALITY PARGASITE

	x	y	z	U_{11}	U_{22}	U_{33}	U_{23}	U_{13}	U_{12}	U_{eq}
O(1)	0.1066(2)	0.0873(1)	0.2167(4)	0.0083(9)	0.0162(9)	0.0090(9)	−0.0010(7)	0.0026(7)	−0.0019(7)	0.0111(6)
O(2)	0.1192(2)	0.1724(1)	0.7319(4)	0.0056(8)	0.0118(9)	0.0101(9)	0.0009(7)	0.0008(7)	0.0000(7)	0.0094(5)
O(3)	0.1068(3)	0	0.7159(5)	0.0057(11)	0.0081(11)	0.0089(13)	0	0.0011(10)	0	0.0077(7)
O(4)	0.3663(2)	1/4	0.7903(4)	0.0123(9)	0.0099(8)	0.0129(10)	−0.0002(7)	0.0050(8)	−0.0019(7)	0.0114(6)
O(5)	0.3505(2)	0.1393(1)	0.1104(4)	0.0086(9)	0.0168(9)	0.0108(10)	0.0045(8)	0.0004(8)	−0.0005(7)	0.0125(6)
O(6)	0.3447(2)	0.1169(1)	0.6098(4)	0.0091(9)	0.0150(9)	0.0135(10)	−0.0046(8)	0.0021(8)	0.0001(7)	0.0127(6)
O(7)	0.3418(3)	0	0.2823(6)	0.0127(14)	0.0120(13)	0.0191(5)	0	0.0026(12)	0	0.0149(9)
T(1)	0.27988(8)	0.08548(4)	0.3030(2)	0.0086(4)	0.0087(3)	0.0084(4)	−0.0001(3)	0.0016(3)	−0.0009(3)	0.0087(2)
T(2)	0.29017(7)	0.17327(4)	0.8125(2)	0.0071(3)	0.0076(3)	0.0069(3)	−0.0004(3)	0.0021(3)	−0.0002(3)	0.0072(2)
M(1)	0	0.08891(7)	1/2	0.0085(6)	0.0097(6)	0.0064(6)	0	0.0023(5)	0	0.0082(4)
M(2)	0	0.17617(6)	0	0.0057(6)	0.0050(6)	0.0048(6)	0	0.0018(5)	0	0.0051(4)
M(3)	0	0	0	0.0071(9)	0.0064(9)	0.0053(9)	0	0.0004(7)	0	0.0065(6)
M(4)	0	0.27942(4)	1/2	0.0117(4)	0.0095(4)	0.0107(4)	0	0.0057(3)	0	0.0101(2)
A(2)	0	0.471(1)	0							0.0200(2)
A(m)	0.045(1)	1/2	0.095(2)							0.0200(2)
H(1)	0.200(2)	0	0.832(8)							0.02

TABLE 3. REFINED SITE-SCATTERING VALUES (*epfu*) AND SITE POPULATIONS
FOR GEM-QUALITY PARGASITE

Site	Refined site-scattering values	Assigned scattering species	Calculated site-scattering	Assigned site-populations	$<M–O>_{calc}$ Å
M(1)	24.5(1)	1.94 Mg* + 0.06 Ti	24.6	1.94 Mg + 0.06 Ti^{4+}	2.076
M(2)	24.4(1)	1.94 Mg* + 0.06 Fe*	24.7	1.40 Mg + 0.54 Al + 0.06 Fe^{3+}	2.04
M(3)	12.1(1)	0.98 Mg* + 0.02 Fe*	12.4	0.81 Mg + 0.17 Al + 0.02 Fe^{2+}	2.047
ΣM(1,2,3)	61.00	–	–	–	–
M(1,2,3)^{EMP}	62.00	–	–	–	–
M(4)	38.4(1)	1.82 Ca + 0.18 Na	38.4	1.82 Ca + 0.18 Na	–
B^{EMP}	38.6	1.86 Ca + 0.14 Na	–	–	–
A(m)	5.8(2)	0.24 K + 0.11 Na	5.8	0.24 K + 0.11 Na	–
A(2)	6.5(2)	0.62 Na	6.8	0.62 Na	–
ΣA	12.3(4)	0.73 Na + 0.24 K	12.6	–	–
A^{EMP}	12.6	–	–	–	–

and an MCT nitrogen-cooled detector; 128 scans were averaged.

Spectrum fitting

The powder- and single-crystal spectra are almost identical (Fig. 1) except for a slight difference in the intensity of the higher-frequency components due to the random orientation of the powder crystallites with respect to the single-crystal fragment. The OH-spectrum of the pargasite shows a rather broad envelope made up of several overlapping bands (Fig. 1). On closer inspection, the spectrum of the Soper River pargasite is very similar to the spectrum of synthetic sample F22 of Robert *et al.* (2000), which is shown in Figure 2 for comparison. The spectrum of Soper River pargasite was fitted using the procedure described in Della Ventura *et al.* (1996). The widths of the component bands were constrained to be approximately equal to the bandwidths in the synthetic (OH,F)-bearing pargasite samples of Robert *et al.* (2000), and the intensities and frequencies (positions) of the components were free to vary. The refinement converged to a model similar to that obtained by Robert *et al.* (2000).

SITE POPULATIONS

The T sites

As Si and Al have very similar X-ray scattering factors, the site occupancies cannot be refined directly from diffraction data, and Al–Si site-populations must be as-

TABLE 4. SELECTED INTERATOMIC DISTANCES (Å) AND ANGLES (°)
FOR GEM-QUALITY PARGASITE FROM SOPER RIVER, BAFFIN ISLAND

T(1)–O(1)		1.652(2)	M(2)–O(1)	x2	2.083(2)
T(1)–O(5)		1.684(2)	M(2)–O(2)	x2	2.070(2)
T(1)–O(6)		1.679(2)	M(2)–O(4)	x2	1.991(1)
T(1)–O(7)		1.667(1)	<M(2)–O>		2.048
<T(1)–O>		1.671			
T(2)–O(2)		1.630(2)	M(3)–O(1)	x4	2.062(2)
T(2)–O(4)		1.589(1)	M(3)–O(3)	x2	2.052(3)
T(2)–O(5)A		1.649(2)	<M(3)–O(3)>		2.057
T(2)–O(6)		1.664(2)			
<T(2)–O>		1.633	M(4)–O(2)	x2	2.414(2)
			M(4)–O(4)	x2	2.336(2)
M(1)–O(1)	x2	2.047(2)	M(4)–O(5)	x2	2.639(2)
M(1)–O(2)	x2	2.094(2)	M(4)–O(6)	x2	2.576(2)
M(1)–O(3)	x2	2.082(2)	<M(4)–O>		2.490
<M(1)–O>		2.074			
			A(2/m)–O(5)	x4	3.040(2)
A(m)–O(5)	x2	3.019(7)	A(2/m)–O(4)	x4	3.060(2)
A(m)–O(5)	x2	3.166(7)	A(2/m)–O(7)	x2	2.430(3)
A(m)–O(6)	x2	2.674(6)	<A(2/m)–O>		2.926
A(m)–O(7)		2.46(1)			
A(m)–O(7)		2.54(1)	A(2)–O(5)	x2	2.63(1)
<A(m)–O>		2.772	A(2)–O(5)	x2	3.48(2)
			A(2)–O(6)	x2	2.73(1)
O(5)–O(6)–O(5)		162.5(1)	A(2)–O(6)	x2	3.44(1)
T(1)–O(5)–T(2)		133.5(1)	A(2)–O(7)	x2	2.485(5)
T(1)–O(6)–T(2)		136.3(1)	<A(2)–O>		2.953
T(1)–O(7)–T(1)		134.2(2)			

A(2/m): 0 ½ 0, with zero occupancy.

TABLE 5. AVERAGE CHEMICAL
COMPOSITION (wt.%)
AND UNIT FORMULA (apfu) OF
GEM-QUALITY PARGASITE

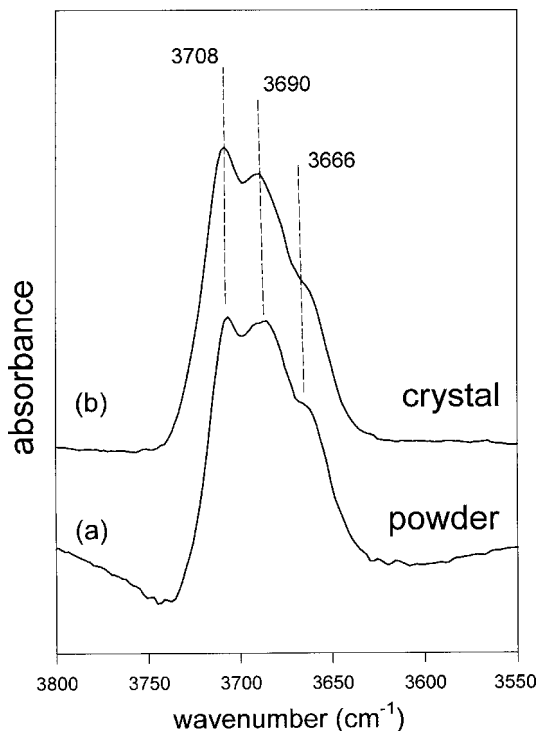|			
SiO_2	45.33	Si	6.45
TiO_2	0.57	Al	1.55
Al_2O_3	13.44	Total	8.00
FeO	0.62		
Cr_2O_3	0.04	Al	0.71
MnO	0.06	Ti	0.06
MgO	19.51	Cr	0.00
CaO	12.05	Fe^{2+}	0.07
Na_2O	3.14	Mg	4.15
K_2O	1.32	Mn	0.01
F	1.41	Total	5.00
H_2O*	1.43		
O=Cl	−0.02	Ca	1.86
O=F	−0.59	Na	0.14
Total	98.29	Total	2.00
		Na	0.73
		K	0.24
		Total	0.97
		OH	1.25
		F	0.63
		O^{2-}	0.12

FIG. 1.   Infrared spectra in the OH-stretching region collected on (a) powder, and (b) a single-crystal fragment of the Soper River pargasite.

signed by taking into account the <T–O> distances and the fact that [4]Si and [4]Al have different empirical radii (0.26 and 0.39 Å, respectively; Shannon 1976). Hawthorne (1983) has derived relations between <T–O> distances and Al–Si site-occupancies. The observed <T(2)–O> distance, 1.633 Å, indicates that the T(2) site is completely occupied by Si. The observed <T(1)–O> distance, 1.671 Å, indicates that Al must be ordered at the T(1) site.

The M(1,2,3) sites

The refined site-scattering values at these sites are close to 24, 24 and 12 *epfu* (electrons per formula unit), respectively, indicating that these sites are dominated by Mg (Z = 12) and Al (Z = 13), as indicated by the unit formula (Table 5). Oberti *et al.* (1992) and Hawthorne *et al.* (1998) have shown that C-group Ti commonly is incorporated into the amphibole structure at the M(1) site, with the locally associated O(3) sites being occupied by O^{2-} rather than the more usual OH or F. There is very little transition-metal content in this amphibole, but the refined site-scattering value for the M(1) site is in exact accord with all Ti occurring at this site. We may test this model by examining the observed <M(1)–O> distance in terms of the aggregate radius of the constituent M(1) cations and the relation between <M(1)–O>, <$r^{M(1)}$> and <$r^{O(3)}$> given by Hawthorne (1983). For Ti^{4+} at M(1), the predicted <M(1)–O> distance is 2.076
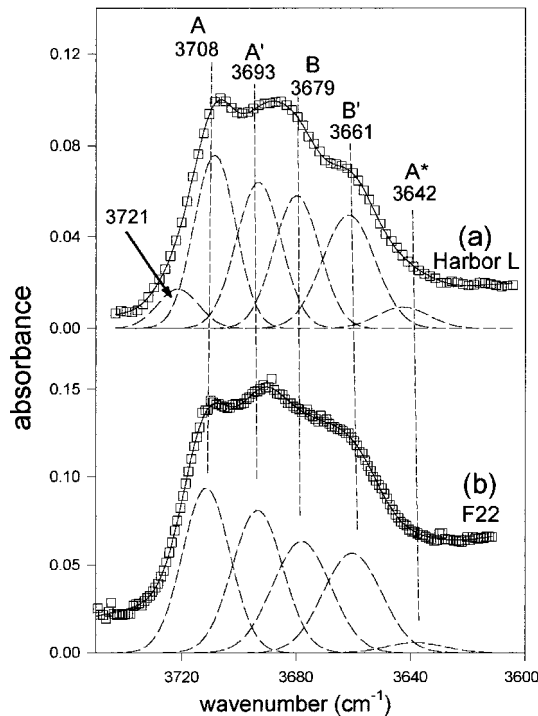
FIG. 2. Comparison of the fitted spectra of (a) Soper River pargasite and (b) synthetic F22 pargasite of Robert *et al.* (2000).

Å; for Fe^{2+} at $M(1)$, the predicted $<M(1)–O>$ distance is 2.080 Å. The observed $<M(1)–O>$ distance is 2.074 Å, in closer agreement with Ti^{4+} occurring at $M(1)$. Moreover, the observed scattering at the $M(1)$ site, 24.5 *epfu* (electrons per formula unit), is in slightly closer agreement with Ti at $M(1)$ (24.6 *epfu*) than with Fe^{2+} at $M(1)$ (24.8 *apfu*). Hence we assign Ti^{4+} to the $M(1)$ site.

For the $M(2)$ and $M(3)$ sites, we may assign Mg* (= Mg + Al) and Fe* (= Fe^{2+} + Mn) according to the observed site-scattering values: $M(2) = 1.94$ Mg* + 0.06 Fe*; $M(3) = 0.98$ Mg* + 0.02 Fe*. To determine the degree of Mg–Al order over $M(2)$ and $M(3)$, we must rely on $<M–O>–<r>$ relations (Hawthorne 1983); this approach is particularly effective for Mg and Al because of the difference in ionic radii: 0.72 *versus* 0.535 Å. The very minor amount of Mn can be included in the amount of Fe^{2+} without any significant discrepancy arising from their difference in size: 0.78 *versus* 0.83 Å for Fe^{2+} and Mn^{2+}, respectively. The amount of Al was adjusted between $M(2)$ and $M(3)$ such that the $<M–O>$ values calculated from the curves of Hawthorne (1983) fit the observed $<M–O>$ distances equally well, *i.e.*, relative to the predicted standard deviations for the curves of Hawthorne (1983). The resulting values are given in Table 3.

The M(4) site

The refined site-scattering value at the $M(4)$ site (Table 3) is compatible with the occupancy of the $M(4)$ site by Ca and Na exactly as indicated by the unit formula determined from the electron-microprobe data (Table 5).

The A sites

The electron density at the *A* sites, calculated with the *A* cations removed from the refinement, is shown in Figure 3. To interpret this pattern of electron density, we will use the results of Hawthorne *et al.* (1996) and the refined site-scattering values of Table 3. First, it is now well established (Hawthorne 1983, Hawthorne *et al.* 1996, and references therein) that K occupies the $A(m)$ site. As the scattering from ^AK is $0.24 \times 19 = 4.6$ *epfu* and the refined scattering at the $A(m)$ site is 5.8 *epfu* (Table 4), Na must occur at both $A(m)$ and $A(2)$ sites. The amounts of cations at these sites may be assigned directly from the refined site-scattering values, as Na is the only other cation present at these sites. The resulting site-populations are shown in Table 3.

Hawthorne *et al.* (1996) showed that ordering of Na over the $A(2)$ and $A(m)$ sites in $C2/m$ clinoamphiboles is associated with local configurations of next-nearest-neighbor cations that seem to be favored over other possible configurations. The most favorable configurations are as follows:

1. $^{M(4)}Na – {}^{O(3)}F – {}^{A(m)}Na$ 0.07

2. $^{M(4)}Ca – {}^{O(3)}OH – {}^{A(2)}Na$ 0.63

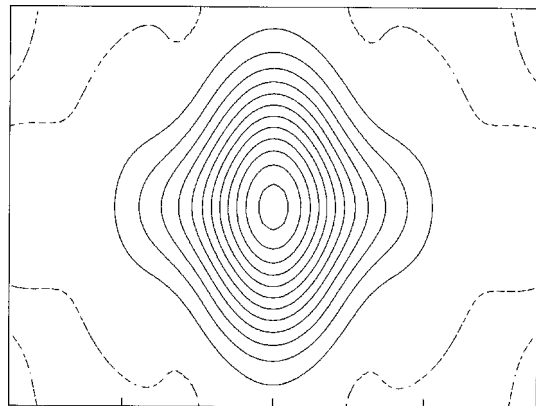3. $^{M(4)}Na – {}^{O(3)}OH – {}^{A(m)}Na$ –

FIG. 3. A difference-Fourier section through the $A(2/m)$ site parallel to (01) and calculated with the *A*-group cations removed from the structure model; the contour interval is 1 $e/Å^3$, and the dashed line is the zero contour.

4. $^{M(4)}Ca - {}^{O(3)}F - {}^{A(m)}Na$ –

5. $^{M(4)}Ca - {}^{O(3)}F - {}^{A(2)}Na$ –

These are listed in terms of decreasing likelihood. Now, we can begin to assign amounts of these configurations from the unit formula (Table 5) of the amphibole, as the amount of each configuration is dictated by the least available of the required components. For configuration (1), the amphibole has 0.14 $apfu$ $^{M(4)}Na$ and 0.63 $apfu$ F, and hence the amount is dictated by the amount of available $^{M(4)}Na$. As there are two $M(4)$ sites to be occupied in this configuration, the fraction of this component present must be 0.07; these values are listed above, next to each configuration. For configuration (2), the amphibole has 1.86 Ca $apfu$ and 1.25 OH pfu, and thus the OH content is the limiting factor. For configuration (2), there are two O(3) sites to be occupied, and hence the fraction of configuration (2) present is 1.25 / 2 = 0.63. For configuration (3), there is no $^{M(4)}Na$ available, and therefore no configuration of this type. Moreover, there are 0.24 local configurations involving K at $A(m)$ and 0.03 involving a vacancy at A. These local configurations sum to 0.97, fairly close to the ideal value of 1.0 pfu.

These configurations also imply specific site-populations at $A(m)$ and $A(2)$. Summing these values, we obtain

$A(m)$ = 0.24 K + 0.14 Na = 6.1 $epfu$

$A(2)$ = 0.63 Na = 6.9 $epfu$

These value agree quite well with the corresponding refined site-scattering values of Table 3, supporting our assignment of short-range-ordered configurations within the structure of this amphibole.

Infrared spectra

The results are compared in Figure 2 to those for a synthetic (OH,F)-bearing pargasite (F22 of Robert et $al.$ 2000). The only significant difference between the two spectra is the presence, in the spectrum of Soper River pargasite, of an additional component at high frequency, indicated by the arrow in Figure 1a. As shown by Robert et $al.$ (1999, 2000), the A and B components (Fig. 2a) can be assigned to local OH–OH arrangements, whereas the A' and B' components can be assigned to local OH–F arrangements. The A^* component, which is present in both spectra (Fig. 2), can be assigned to a partly vacant A-site (Della Ventura et $al.$ 1999). The higher-frequency band at 3721 cm^{-1}, resolved in the spectrum of Soper River pargasite (Fig. 1a), can be assigned to OH locally associated with Si–O(7)–Si linkages (Della Ventura et $al.$ 1999). This is compatible with a slight excess of Si (Si > 6.0 $apfu$), in agreement with the unit formula (Table 5). From the relative intensities

of the A–A' and B–B' doublets, we derive an anion composition close to $(OH)_{1.20}F_{0.80}$, in reasonable accord with the anion content of the unit formula, $(OH)_{1.25}F_{0.63}O_{0.12}$ (Table 5). Calculation of the number of MgMgMg : MgMgAl configurations [$i.e$, the Mg:Al contents of the $M(3)$ site] gives 0.65:0.35 compared with the SREF value of 0.83:0.17 (Table 3). This discrepancy is not unreasonable considering the complexity of this amphibole; the spectrum is in accord with the partial disorder of Al over the $M(2)$ and $M(3)$ sites.

PARAGENESIS

This pargasite from Baffin Island is very similar in composition to a suite of pargasite samples characterized by Oberti et $al.$ (1995). Amphiboles from both localities show disorder of $^{[6]}Al$ over the $M(2)$ and $M(3)$ sites, and hence it is of interest to compare the geology and conditions of formation of both of these occurrences.

Baffin Island

The Quebec–Baffin segment of Trans-Hudson Orogen consists of tectonostratigraphic elements accumulated on, or accreted to, the northern margin of the Archean Superior Province during more than 200 m.y. of divergent- and convergent-margin tectonic activity (St-Onge et $al.$ 1992). Underlying much of the orogen (St-Onge et $al.$ 1996, 1998, 1999) are: (i) lower-plate parautochthonous plutonic and supracrustal rocks of the Archean Superior Province, and (ii) parautochthonous sedimentary and volcanic cover units (Povungnituk and Chukotat groups) associated with multiple rifting of the Superior Province at 2.04 and 1.92 Ga.

Structurally overlying the parautochthonous units are upper-plate ($i.e.$, allochthonous) Paleoproterozoic crustal elements interpreted as an ophiolite (Watts Group) [2.00 Ga], containing (i) a fore-arc clastic apron, (ii) a magmatic arc (Parent Group and Narsajuaq arc) [1.86–1.82 Ga] and arc-derived detritus (Sugluk Group), (iii) a clastic-carbonate platform-sequence (Lake Harbour Group) and its potential basement (Ramsay River orthogneiss), (iv) a foreland-basin (?) sequence (Blandford Bay assemblage), and (v) an extensive suite of monzogranitic plutons (Cumberland batholith) [1.86 and 1.85 Ga] that intrude rocks of both the platform and the foreland basin.

Pargasite occurs in the supracrustal rocks of the Lake Harbour Group. The assemblages of metamorphic minerals in the Lake Harbour Group and the Blanford Bay assemblage are indicative of a largely retrograde transition from granulite to amphibole facies. Metamorphic minerals in the siliceous marbles of the Lake Harbour Group include diopside, phlogopite, humite, wollastonite, spinel, forsterite and tremolite.

Arc-related granulite-facies metamorphism predates collision-related amphibolite-facies metamorphism in

the Quebec–Baffin segment of the Trans-Hudson Orogen, and all granulite- to amphibolite-facies transitions in this segment of the orogen (*i.e.*, within the lower-plate Superior Province basement, and upper-plate Narsajuaq arc, Sugluk Province, Lake Harbour Group and Blandford Bay assemblage) can be interpreted as retrograde in origin, with the amphibolite-facies overprint occurring up to hundreds of millions of years after the initial granulite-facies metamorphism. Preliminary thermobarometric work on thermal peak assemblages from the Lake Harbour Group and Blandford Bay assemblage indicates conditions of *ca.* 800ºC and <7 kbar, consistent with the mineral assemblages observed in the field (St-Onge *et al.* 2000).

Finero

The Finero Complex of northwestern Italy and southern Switzerland is a phlogopite-bearing mantle-peridotite massif surrounded by an intrusive sequence of gabbros and (possibly cogenetic) cumulate peridotites (Lu *et al.* 1997). It occurs within high-grade metasediments (kinzigites, stronalites) and metavolcanic rocks, and consists, from the core outward, of an amphibole- and phlogopite-bearing peridotite, a layered internal zone of ultramafic and mafic rocks, an amphibole peridotite and an external gabbro. The phlogopite peridotite unit, whose thickness is unknown, forms an elongate body at the core of the Finero complex. Its main distinct lithology is amphibole- and phlogopite-bearing harzburgite. Patches of dunite are common and generally form irregularly shaped bodies that are associated with chromitite. The layered internal zone consists of cyclic units of amphibole websterite, amphibole peridotite, garnet–amphibole gabbro and anorthosite. The increasing content of modal olivine marks a transition from the layered internal zone to the amphibole peridotite. The unit consists of dunite, wehrlite and lherzolite enriched in pargasitic amphibole. Thin layers of chromian spinel and patches of coarse-grained pargasite are found locally in this unit. Siena & Coltorti (1989) concluded that amphibole is an important liquidus phase in the Finero complex, and suggested that crystallization took place at 1000°C and 10 kbar.

Baffin Island and Finero

Conditions of amphibole formation at these two localities are ~800°C and <7 kbar and ~1000°C and ~10 kbar. These conditions are significantly different and yet the patterns of Al–Mg order in the constituent amphiboles are very similar. This similarity supports the conclusion of Oberti *et al.* (1995) that (Mg,Al) disorder in pargasite at Finero is induced by the chemical composition of the amphibole, rather than the high temperature and pressure of formation.

REFERENCES

DELLA VENTURA, G., HAWTHORNE, F.C., ROBERT, J.-L., DELBOVE, F., WELCH, M.D. & RAUDSEPP, M. (1999): Short-range order of cations in synthetic amphiboles along the richterite–pargasite join. *Eur. J. Mineral.* **11**, 79-94.

_____, ROBERT, J.-L., HAWTHORNE, F.C. & PROST, R. (1996): Short-range disorder of Si and Ti in the tetrahedral double-chain unit of synthetic Ti-bearing potassium-richterite. *Am. Mineral.* **81**, 56-60.

GRICE, J.D. & GAULT, R.A. (1983): Lapis lazuli from Lake Harbour, Baffin Island, Canada. *Rocks and Minerals* **58**, 12-19.

HAWTHORNE, F.C. (1983): The crystal chemistry of the amphiboles. *Can. Mineral.* **21**, 173-480.

_____, OBERTI, R. & SARDONE, N. (1996): Sodium at the A site in clinoamphiboles: the effects of composition on patterns of order. *Can. Mineral.* **34**, 577-593.

_____, _____, ZANETTI, A. & CZAMANSKE, G.K. (1998): The role of Ti in hydrogen-deficient amphiboles: sodic-calcic and sodic amphiboles from Coyote Peak, California. *Can. Mineral.* **36**, 1253-1265.

LU, MEIHUA, HOFMANN, A.W., MAZZUCCHELLI, M. & RIVALENTI, G. (1997): The mafic-ultramafic complex near Finero (Ivrea–Verbano Zone). I. Chemistry of MORB-like magmas. *Chem. Geol.* **140**, 207-222.

OBERTI, R., HAWTHORNE, F.C., UNGARETTI, L. & CANNILLO, E. (1995): $^{[6]}$Al disorder in amphiboles from mantle peridotites. *Can. Mineral.* **33**, 867-878.

_____, UNGARETTI, L., CANNILLO, E. & HAWTHORNE, F.C. (1992): The behaviour of Ti in amphiboles. I. Four- and six-coordinate Ti in richterite. *Eur. J. Mineral.* **3**, 425-439.

ROBERT, J.-L., DELLA VENTURA, G. & HAWTHORNE, F.C. (1999): Near infrared study of short-range disorder of OH and F in monoclinic amphiboles. *Am. Mineral.* **84**, 86-91.

_____, _____ & THAUVIN, J.-L. (1989): The infrared OH-stretching region of synthetic richterites in the system

Na$_2$O–K$_2$O–CaO–MgO–SiO$_2$–H$_2$O–HF. *Eur. J. Mineral.* **1**, 203-211.

_____, _____, WELCH, M.D. & HAWTHORNE, F.C. (2000): The OH–F substitution in synthetic pargasite at 1.5 kbar, 850°C. *Am. Mineral.* **85**, 926-931.

SHANNON, R.D. (1976): Revised effective ionic radii and systematic studies of interatomic distances in halides and chalcogenides. *Acta Crystallogr.* **A32**, 751-767.

SIENA, F. & COLTORTI, M. (1989): The petrogenesis of a hydrated mafic-ultramafic complex and the role of amphibole fractionation at Finero (Italian Western Alps). *Neues Jahrb. Mineral., Monatsh.*, 255-274.

ST-ONGE, M.R., HANMER, S. & SCOTT, D.J. (1996): Geology of the Meta Incognita Peninsula, south Baffin Island, Northwest Territories: tectonostratigraphic units and regional correlations. *Geol. Surv. Can., Pap.* **1996-C**, 63-72.

_____, LUCAS, S.B. & PARRISH, R.R. (1992): Terrane accretion in the internal zone of the Ungava orogen, northern Quebec. 1. Tectonostratigraphic assemblages and their tectonic implications. *Can. J. Earth Sci.* **29**, 746-764.

_____, _____, SCOTT, D.J. & WODICKA, N. (1999): Upper and lower-plate juxtaposition, deformation and metamorphism during crustal convergence, Trans-Hudson Orogen (Quebec–Baffin segment), Canada. *Precamb. Res.* **93**, 27-49.

_____, SCOTT, D.J., WODICKA, N. & LUCAS, S.B. (1998): Geology of the McKellar Bay – Wight Inlet – Frobisher Bay area, southern Baffin Island, Northwest Territories. *Geol Surv. Can., Pap.* **1998-C**, 43-53.

_____, WODICKA, N. & LUCAS, S.B. (2000): Granulite- and amphibolite-facies metamorphism in a convergent-plate-margin setting: synthesis of the Quebec–Baffin segment of the Trans-Hudson Orogen. *Can. Mineral.* **38**, 379-398.

WIGHT, W. (1986): Gem hornblende from Baffin Island, NWT, Canada. *J. Gemmology* **20**, 100-107.